Metric Exploitation of a Single Low Oblique Aerial Image

Styliani VERYKOKOU and Charalabos IOANNIDIS, Greece

SUMMARY

In recent years, oblique aerial images are involved in various photogrammetric processes and are used not only for interpretation or visualization purposes but also in metric applications. This paper describes an approach for the computation of vertical and horizontal distances from a single low oblique aerial image. The proposed methodology can be applied in the case where the camera exterior orientation is unknown. It relies on the automatic determination of the nadir point using edge detection and line extraction algorithms, combined with robust model fitting and least-squares techniques, taking into account the underlying geometry of oblique imagery. The workflow and the mathematical model used are presented in detail and the effect of different variables (flying height, camera constant, tilt of the camera axis, length of the line segment, error in the determination of the flying height and error due to lack of ground elevation information) on the errors of both measured vertical and horizontal distances is evaluated. Finally, the desktop application that was developed based on the proposed methodology and tested using a data set of low oblique imagery is presented and ideas for future research are discussed.

Metric Exploitation of a Single Low Oblique Aerial Image (7516)   1/16
Styliani Verykokou and Charalabos Ioannidis (Greece)

FIG Working Week 2015
From the Wisdom of the Ages to the Challenges of the Modern World
Sofia, Bulgaria, 17-21 May 2015

Metric Exploitation of a Single Low Oblique Aerial Image

Styliani VERYKOKOU and Charalabos IOANNIDIS, Greece

1. INTRODUCTION

For many decades in the past, the photogrammetric process of extracting accurate geometric information was based almost solely on vertical aerial imagery. However, the history of aerial photography dates back to 1839 when Daguerre took the first oblique aerial image from the top of a tall building in Paris, while the subsequent aerial photographs were also oblique and were extensively used for mapping and reconnaissance purposes (Hannavy, 2007; Petrie, 2008; Baumann, 2014). In recent years, oblique aerial images have come back to the foreground, not only as a complementary dataset to traditional vertical airborne images, but also as the basic source of information for various kinds of applications.

Oblique aerial images are taken with the camera axis intentionally inclined with respect to the vertical. They are characterized as either high oblique, if they are tilted sufficiently to show the horizon, or low oblique, if they do not include the horizon (Moffitt and Mikhail, 1980; Wolf, 1983). Today, aerial platforms equipped with multiple cameras that take both vertical and oblique photographs are used by several companies and organizations that exploit the strengths of both types of imagery and gradually encompass oblique images into various photogrammetric processes. Apart from the provision of a complementary dataset to vertical photographs, they can also be used independently, as the basic data source for various kinds of applications, including 3D modeling, digital monoplotting, scene interpretation and classification for cadastral, military as well as infrastructural projects (Grenzdörffer et al., 2008; Gerke, 2013). Some of the fundamental characteristics of oblique photographs are their trapezoidal footprint, the big change of scale, the coverage of a larger ground area compared to vertical images taken from the same altitude by the same camera, the possibility they offer for the photographic coverage of areas over which it is impossible to carry out a flight and the intuitive interpretation by people, because they are accustomed to seeing ground features with a similar perspective (Fahsi, 1996).

The metric exploitation of oblique aerial images is an issue of major significance for many applications, including 3D cadastre projects (measurements of both vertical and horizontal sides of buildings, extraction of building volumes, etc.), urban planning, real estate, property management, cultural heritage documentation and even more. Several companies are involved in the acquisition of oblique aerial images, in addition to vertical ones, and in the provision of software that allows users to make measurements on them, using the camera exterior orientation information as well as ground elevation data. However, is it possible to retrieve metric information from a single oblique photograph with unknown exterior orientation? What is the impact on the accuracy if no elevation information is available? The purpose of this paper is the presentation of a workflow for making measurements of vertical and horizontal distances from single low oblique aerial images, without knowledge of the camera six-degrees-of-freedom pose, as well as the investigation of the accuracy that can be achieved.

2. METHODOLOGY

In this section, the proposed methodology for the extraction of vertical and horizontal distances from a single low oblique aerial image is presented.

2.1 Input Data

The prerequisites for the implementation of the methodology that is proposed are:
− a low oblique aerial image on which horizontal and vertical line segments (e.g., limits of parcels, edges of buildings, poles, etc.) are clearly visible,
− the interior orientation of the camera that was used to capture the image,
− the flying height of the aerial platform and
− in the case of measuring a vertical distance: the difference in elevation between the ground nadir (i.e., the point on the ground vertically underneath the perspective center of the camera lens system) and the point at the bottom of the vertical object
− in the case of measuring a horizontal distance: the difference in elevation between the ground nadir and the endpoints of the horizontal line segment to be measured.

Practically, an average elevation difference between the region under the aerial platform and the region of interest depicted in the oblique photograph suffices for the metric exploitation of an oblique image. However, this is a quantity that is usually unknown. It can be either estimated, using a free to download Global Digital Elevation Model (GDEM) or elevation information taken from a program like Google Earth, or even assumed to be zero.

2.2 Automatic Nadir Point Detection

The most important step for the metric exploitation of an oblique aerial image is the detection of the nadir point, that is, the intersection between the vertical line from the perspective center and the oblique image plane. This is the vanishing point of the vertical direction and may lie outside the oblique image limits (Fig. 1). The proposed methodology for its automatic detection is presented below.

2.2.1 Undistortion of the image

First step is the correction of the lens distortion effect over the oblique image, using the calibration output of the airborne camera, to wit, the pixel coordinates of the principal point, the camera constant and the coefficients of radial and tangential lens distortion polynomials, according to the Brown-Conrady model (Brown, 1971). The undistorted image is used for the automatic detection of the nadir point and this is the image on which photogrammetric measurements of distances are made.

2.2.2 Automatic detection of the true horizon line

The true horizon line is the intersection between the horizontal plane containing the perspective center and the oblique image plane (Fig. 1). All the horizontal line segments converge to this line, which lies outside a low oblique image. Since the horizontal structures

in a low oblique image usually stand out more than the vertical ones, the true horizon detection using horizontal lines is an essential step for the acquisition of an initial estimation of the nadir point, before its final determination through convergence of vertical lines. The process for the automatic detection of the true horizon line is described below.

The Canny edge detector (Canny, 1986) is used for the extraction of edges in the undistorted image, after it is converted to greyscale. Subsequently, the Progressive Probabilistic Hough Transform (Matas et al., 1998) is applied in the binary edge map obtained using the Canny operator for the extraction of line segments in the oblique image.

Next step is the detection of the vanishing points of two horizontal directions. Firstly, a variation of the RANSAC (RANdom SAmple Consensus) algorithm (Fischler and Bolles, 1981) is applied for the estimation of the intersection point of most horizontal line segments, relying on the use of two line segments. In this variation, the iterative random choice of two line segments is controlled, so that the initial estimation of their intersection point lies outside the image limits, having a negative y coordinate (assuming that the origin of the image coordinate system is located at the top left corner, positive x-axis points to the right and positive y-axis is directed downward). Then, a generalized least-squares adjustment technique for nonlinear condition equations is implemented for the iterative calculation of the vanishing point, using its initial estimation obtained by RANSAC as well as the inliers which converge to this point, returned by the same algorithm. Subsequently, the horizontal line segments that converge to the first detected vanishing point are removed from the set of all line segments and the same procedure is repeated, for the detection of a second horizontal vanishing point. The line that connects these two vanishing points is the true horizon line.
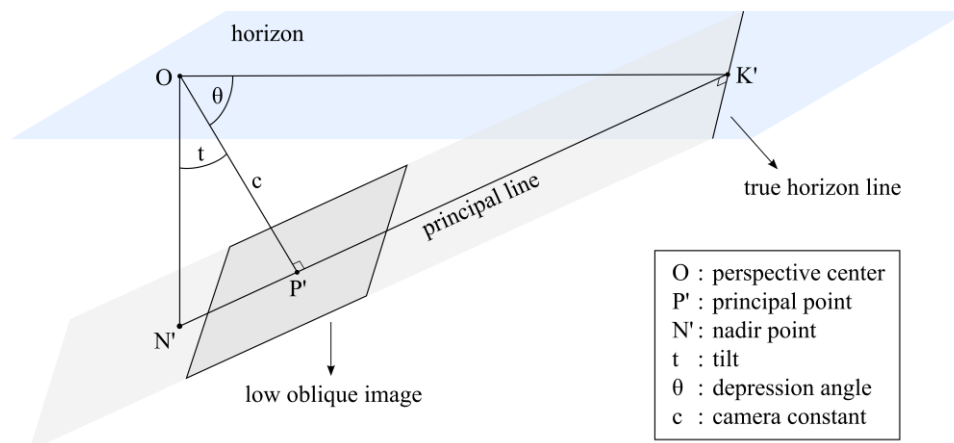
Figure 1. Geometry of a low oblique aerial image

2.2.3 Initial estimation of the nadir point

First step for the initial estimation of the nadir point is the determination of the principal line, that is, the intersection of the plane which includes the optical axis and the vertical line from the perspective center (principal plane) with the oblique image. This line passes through the nadir point and the principal point and it is the line of maximum tilt in an oblique image (Fig. 1). After the true horizon detection, the equation of the principal line is determined, based on

Metric Exploitation of a Single Low Oblique Aerial Image (7516)   4/16
Styliani Verykokou and Charalabos Ioannidis (Greece)

FIG Working Week 2015
From the Wisdom of the Ages to the Challenges of the Modern World
Sofia, Bulgaria, 17-21 May 2015

the fact that it is perpendicular to the true horizon line and passes through the principal point.

Then, the position of the intersection point K' between the true horizon line and the principal line is calculated and its distance from the principal point is computed, since both points have known coordinates. The depression angle θ, that is, the angle between the horizontal plane containing the perspective center and the optical axis, is calculated according to equation (1).

$$\theta = \arctan\left(\frac{P'K'}{c}\right) \tag{1}$$

Then, the distance between the principal point and the nadir point is calculated according to equation (2), as the angle of depression is the complement of tilt (Fig. 1).

$$P'N' = c \cdot \tan t \quad \rightarrow \quad P'N' = c \cdot \cot\theta \tag{2}$$

The coordinates of the nadir point are determined using the calculated distance $P'N'$ as well as the coordinates of the principal point and taking into consideration the fact that the nadir point lies on the principal line. The resulting system of two equations has two solutions for the coordinates of the nadir point; however, only the solution according to which the nadir point is located below the principal point, thus having a greater y-coordinate, is correct. In this way, an initial estimation of the nadir point position is obtained. It is not considered to be the final one, as the errors arising from the calculation of the two horizontal vanishing points are involved in this estimation of the nadir point according to the presented methodology.

2.2.4 Final estimation of the nadir point

First step of this process is the detection of Canny edges in the oblique image, using a lower "high threshold" as well as a lower "low threshold", compared to the thresholds defined for the extraction of edges in order to detect horizontal vanishing points. This choice is made so that more line segments are detected, in order to ensure that vertical edges will also be extracted in addition to horizontal ones. These two thresholds are used by the Canny operator in its hysteresis thresholding step, according to which if the gradient of a pixel is higher than the high threshold, it is accepted as an edge; if it is below the low threshold, it is rejected; if it is between these two thresholds, it is accepted in the case where it is connected to a pixel with a gradient above the high threshold.

Then, the Progressive Probabilistic Hough Transform is applied for the extraction of line segments. If the distance of the initial estimation of the nadir point from the line that passes through the endpoints of a line segment is above a maximum accepted value, the segment is not considered to be vertical and it is rejected. The remaining line segments are passed to a variation of the RANSAC algorithm, according to which the random iterative choice of two line segments is controlled, so that their intersection point lies close to the initial estimation of the nadir point. The final estimation of the nadir point is obtained through least-squares adjustment, using all the line segments that converge to the initial estimation of the nadir point, returned by RANSAC.

Metric Exploitation of a Single Low Oblique Aerial Image (7516)   5/16
Styliani Verykokou and Charalabos Ioannidis (Greece)

FIG Working Week 2015
From the Wisdom of the Ages to the Challenges of the Modern World
Sofia, Bulgaria, 17-21 May 2015

2.3 Calculation of Vertical and Horizontal Distances

The calculation of the coordinates of the nadir point of an oblique image permits the extraction of metric information. In this section, the mathematical models used for the determination of both vertical and horizontal distances from a single low oblique image are presented.

2.3.1   Mathematical model used for the determination of vertical distances

The derivation of the formula for the calculation of the height of a vertical object is presented below. In Fig. 2, B' and T' are the images of the bottom point B and the top point T, respectively, of an edge of a vertical object that is being measured photogrammetrically from a low oblique aerial image. H indicates the flying height, while ΔH is the elevation difference between the ground nadir point N and the bottom point of the vertical object.
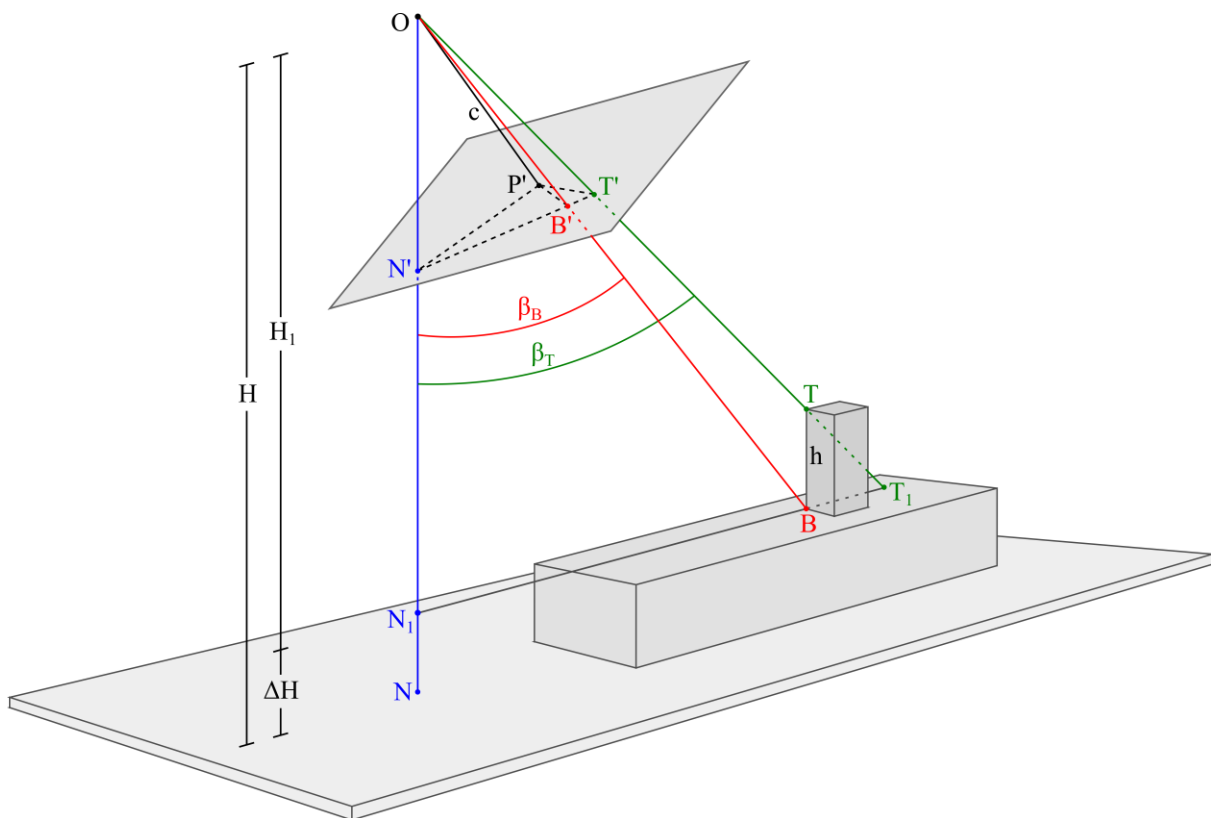

Figure 2. Height determination from a low oblique image

Using the similar triangles ON_1T_1 and TBT_1, the height of the vertical object is calculated according to equation (3).

$$h = \frac{H_1 \cdot BT_1}{N_1T_1} \qquad (3)$$

The distance BT_1 is computed by equation (4).

$$BT_l = N_l T_l - N_l B \;\rightarrow\; BT_l = H_l \tan\beta_T - H_l \tan\beta_B \;\rightarrow\; BT_l = H_l\left(\tan\beta_T - \tan\beta_B\right) \quad (4)$$

The elevation difference between the perspective center and the bottom point of the vertical object is calculated according to equation (5).

$$H_l = H - \Delta H \tag{5}$$

The combination of equations (3), (4) and (5) gives the height of the vertical object (equation 6).

$$h = \left(H - \Delta H\right)\left(1 - \frac{\tan\beta_B}{\tan\beta_T}\right) \tag{6}$$

The cosine of the angle β_B between the vertical line from the perspective center and the optical ray to the bottom point of the vertical object is calculated according to equation (7), by applying the law of cosines in the triangle $OB'N'$.

$$\cos\beta_B = \frac{\left(OB'\right)^2 + \left(ON'\right)^2 - \left(B'N'\right)^2}{2\left(OB'\right)\left(ON'\right)} \tag{7}$$

The tangent of this angle is computed by equation (8).

$$\tan\beta_B = \frac{\sqrt{1-\cos^2\beta_B}}{\cos\beta_B} \;\rightarrow\; \tan\beta_B = \frac{\sqrt{4\left(OB'\right)^2\left(ON'\right)^2 - \left[\left(OB'\right)^2 + \left(ON'\right)^2 - \left(B'N'\right)^2\right]^2}}{\left(OB'\right)^2 + \left(ON'\right)^2 - \left(B'N'\right)^2} \tag{8}$$

The tangent of the angle β_T between the vertical line from the perspective center and the optical ray to the top point of the vertical object is calculated in a similar way, according to equation (9).

$$\tan\beta_T = \frac{\sqrt{4\left(OT'\right)^2\left(ON'\right)^2 - \left[\left(OT'\right)^2 + \left(ON'\right)^2 - \left(T'N'\right)^2\right]^2}}{\left(OT'\right)^2 + \left(ON'\right)^2 - \left(T'N'\right)^2} \tag{9}$$

Equations (10), (11) and (12) are derived by the Pythagorean Theorem applied to the right triangles $OP'B'$, $OP'T'$ and $OP'N'$ respectively.

$$ON' = \sqrt{c^2 + \left(P'N'\right)^2} \tag{10}$$

$$OB' = \sqrt{c^2 + \left(P'B'\right)^2} \tag{11}$$

$$OT' = \sqrt{c^2 + \left(P'T'\right)^2} \tag{12}$$

Finally, the height of a vertical object is calculated according to equations (6), (8), (9), (10), (11) and (12), using the following formula (equation (13)).

$$h = (H - \Delta H) \left(1 - \frac{\dfrac{\sqrt{4\left(c^2 + (P'B')^2\right)\left(c^2 + (P'N')^2\right) - \left[2c^2 + (P'B')^2 + (P'N')^2 - (B'N')^2\right]^2}}{2c^2 + (P'B')^2 + (P'N')^2 - (B'N')^2}}{\dfrac{\sqrt{4\left(c^2 + (P'T')^2\right)\left(c^2 + (P'N')^2\right) - \left[2c^2 + (P'T')^2 + (P'N')^2 - (T'N')^2\right]^2}}{2c^2 + (P'T')^2 + (P'N')^2 - (T'N')^2}} \right)$$

$$\begin{aligned}
(P'B')^2 &= (x_{B'} - x_{P'})^2 + (y_{B'} - y_{P'})^2 \\
(P'N')^2 &= (x_{N'} - x_{P'})^2 + (y_{N'} - y_{P'})^2 \\
(B'N')^2 &= (x_{N'} - x_{B'})^2 + (y_{N'} - y_{B'})^2 \quad \text{where} \\
(P'T')^2 &= (x_{T'} - x_{P'})^2 + (y_{T'} - y_{P'})^2 \\
(T'N')^2 &= (x_{N'} - x_{T'})^2 + (x_{N'} - y_{T'})^2
\end{aligned}$$

$\left\{ \begin{array}{l} x_{B'},\, y_{B'},\, x_{T'},\, y_{T'}: \\ \text{the undistorted image coordinates of} \\ \text{the bottom and the top point of the} \\ \text{vertical object} \\ \\ x_{N'},\, y_{N'}: \\ \text{the undistorted image coordinates} \\ \text{of the nadir point} \\ \\ x_{P'},\, y_{P'}: \\ \text{the coordinates of the principal point} \end{array} \right\}$ (13)

h: the height of the vertical object being measured

H: the flying height

ΔH : the height difference between the ground nadir and the bottom of the vertical object

  $\Delta H > 0$ if the ground nadir is lower in elevation than the bottom of the vertical object

  $\Delta H < 0$ if the ground nadir is higher in elevation than the bottom of the vertical object

2.3.2 Mathematical model used for the determination of horizontal distances

The calculation of horizontal distances from an oblique aerial image requires the use of both an auxiliary image coordinate system and a ground coordinate system. The origin of the auxiliary image coordinate system is located at the nadir point; y axis coincides with the principal line and x axis is perpendicular to it, thus being a horizontal line (Fig. 3). It is proved that the coordinates of an image point A' in this system are calculated according to equations (14) (Wolf, 1983).

$$\begin{aligned}
x'_{A'} &= x^c_{A'} \cos \varphi - y^c_{A'} \sin \varphi \\
y'_{A'} &= x^c_{A'} \sin \varphi + y^c_{A'} \cos \varphi + c \tan t
\end{aligned}$$
(14)

where the rotation angle φ is: $\varphi = s - 180^o$ and s is the swing angle, measured clockwise from the positive y^c axis to the principal line at the nadir point. The angle φ is calculated geometrically, after the determination of the point of intersection between the x axis and the principal line, which is computed using the principal point and the nadir point (Fig. 3).

The coordinates of A' in the image coordinate system centered at the principal point (x^c, y^c) are calculated using their corresponding undistorted coordinates and the position of the principal point in the image coordinate system with the origin at the top left pixel. Hence, the auxiliary image coordinates of a ground point A are calculated by equations (15).

Metric Exploitation of a Single Low Oblique Aerial Image (7516)   8/16
Styliani Verykokou and Charalabos Ioannidis (Greece)

FIG Working Week 2015
From the Wisdom of the Ages to the Challenges of the Modern World
Sofia, Bulgaria, 17-21 May 2015

$$x'_{A'} = \left(x_{A'} - x_{P'}\right)\cos\varphi - \left(y_{P'} - y_{A'}\right)\sin\varphi$$

$$y'_{A'} = \left(x_{A'} - x_{P'}\right)\sin\varphi + \left(y_{P'} - y_{A'}\right)\cos\varphi + P'N'$$
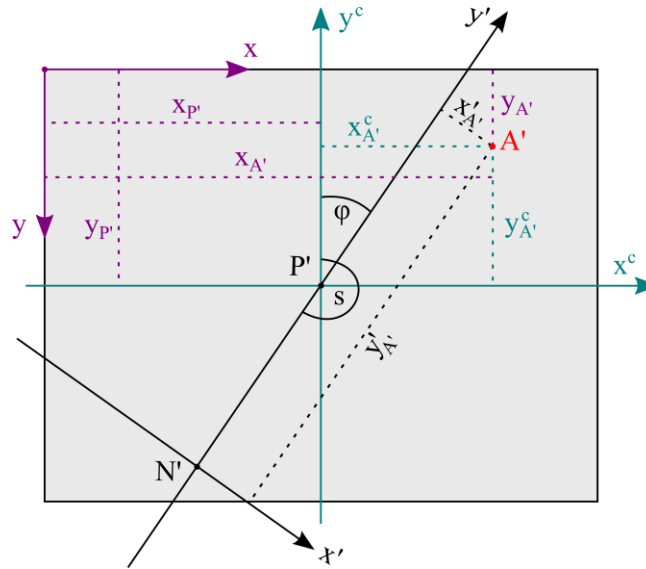
(15)

Figure 3. Auxiliary coordinate system in a low oblique image

The auxiliary ground coordinate system has its origin at the datum nadir point, while X' and Y' axes lie on the same vertical planes with the axes of the auxiliary image coordinate system, being positive in the same directions as them (Moffitt and Mikhail, 1980; Wolf, 1983). Figure 4 illustrates the calculation of the auxiliary ground coordinates of a point A, where: A_1 is the projection of A on the vertical plane that contains Y' axis,

A'_1 is the projection of A' on auxiliary x' axis, thus being the image of A_1, and

line A'_1D' is perpendicular to the vertical line from the perspective center.

Equation (16) is derived using the similar triangles $OA'A'_1 - OAA_1$ and $OD'A' - ON_1A$.

$$\frac{A'A'_1}{AA_1} = \frac{OD'}{ON_1} \;\rightarrow\; \frac{x'_{A'}}{X'_A} = \frac{ON' - D'N'}{H - \Delta H}$$

(16)

The ground X' coordinate of A is calculated according to equation (17), which is derived using equation (16) and by applying trigonometric relations in the right triangles $OP'N'$ and $D'A'_1N'$.

$$X'_A = \frac{\left(H - \Delta H\right)x'_{A'}}{\dfrac{c}{\cos t} - y'_{A'}\sin t} \;\rightarrow\; X'_A = \frac{\left(H - \Delta H\right)x'_{A'}\cos t}{c - y'_{A'}\sin t \cos t}$$

(17)

The ground Y' coordinate of A is calculated by equation (18) in a similar way, by using the similar triangles $OD'A'_1 - ON_1A_1$ and the right triangle $D'A'_1N'$.

$$\frac{y'_A \cdot \cos t}{Y'_A} = \frac{\dfrac{c}{\cos t} - y'_A \cdot \sin t}{H - \Delta H} \quad \rightarrow \quad Y'_A = \frac{(H - \Delta H) \, y'_A \cdot \cos^2 t}{c - y'_A \cdot \sin t \cos t} \tag{18}$$
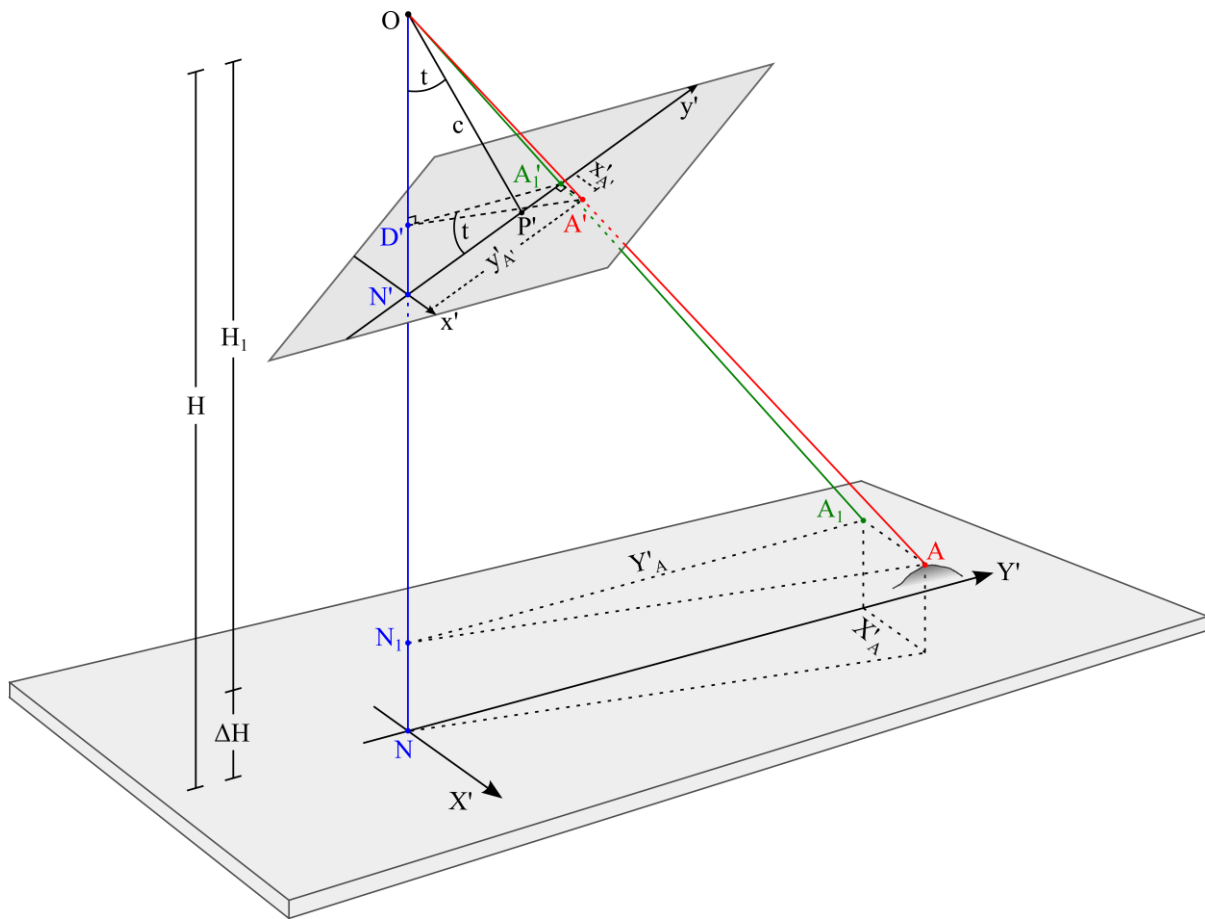

Figure 4. Calculation of ground coordinates from a low oblique image

Hence, the calculation of the distance between two points A and C, which are measured in the undistorted image, includes the following steps:

– geometric determination of the angle φ,
– calculation of the tilt angle, according to equation (2),
– calculation of the auxiliary image coordinates of A and C ($x'_{A'}$, $y'_{A'}$, $x'_{C'}$, $y'_{C'}$), according to equations (15),
– calculation of the auxiliary ground coordinates of A and C (X'_A, Y'_A, X'_C, Y'_C), according to equations (17) and (18), and
– computation of the distance d between A and C, using equation (19).

$$d = \sqrt{\left(X'_C - X'_A\right)^2 + \left(Y'_C - Y'_A\right)^2} \tag{19}$$

3. ASSESSMENT OF ERRORS

The variables that may affect the accuracy of the measurement of a vertical or a horizontal distance, due to their values and errors, are the following:
- the flying height,
- the elevation difference ΔH,
- the relative image positions of the two points being measured, which determine the length of their distance,
- the camera interior orientation parameters and
- the position of the nadir point in the image, which depends on the tilt of the camera axis and the camera constant.

Assuming that:
- the camera interior orientation is known with very high accuracy (thus setting the errors of the principal point, the camera constant and the distortion coefficients to zero),
- the measurements of the image points are very accurate (considering an error of 0.5 pixel in the measured coordinates of each point),
- the nadir point is accurately determined (considering an error of 10 pixels in both x and y coordinates of the nadir point)

and considering a camera resolution of 60 MP and a pixel size of 6 μm, the standard errors of the measured vertical and horizontal distances were calculated by error propagation for the following four case studies.
- Case study 1: σ_H=0.5 m and $\sigma_{\Delta H}$=0.15 m; the flying height H is accurately known and the elevation difference ΔH is either known with high accuracy (if precise elevation data are available for the region under the aerial platform and the region of interest) or set to zero, provided that the ground is relatively flat.
- Case study 2: σ_H=0.5 m and $\sigma_{\Delta H}$=10 m; the flying height H is accurately known and ΔH is either roughly estimated (e.g., by using a free program like Google Earth) or set to zero, assuming small variations in ground elevations.
- Case study 3: σ_H=15 m and $\sigma_{\Delta H}$=0.15 m; H is approximately estimated and ΔH is known with high accuracy.
- Case study 4: σ_H=15 m and $\sigma_{\Delta H}$=10 m.

For all the above case studies, different combinations of the camera constant (50 mm and 150 mm), the tilt angle (15º and 35º) and the flying height (200 m, 500 m and 1000 m) were applied. The resulting standard errors are presented in Tables 1 and 2, for vertical distances ranging from 3 m to 40 m and horizontal distances ranging from 10 m to 90 m respectively.

The following conclusions may be derived:
- An increase in the camera constant and in the tilt of the camera axis leads to higher accuracy in height measurements.
- The standard error of a horizontal distance is almost independent from the camera constant and the tilt angle.
- An increase in the error of the flying height and in the error of the elevation difference ΔH generally increases the error of both vertical and horizontal distances. An increase in the flying height reduces the effect of these errors on the standard error of the distance being measured.

Metric Exploitation of a Single Low Oblique Aerial Image (7516)   11/16
Styliani Verykokou and Charalabos Ioannidis (Greece)

FIG Working Week 2015
From the Wisdom of the Ages to the Challenges of the Modern World
Sofia, Bulgaria, 17-21 May 2015

– The standard error of a greater vertical and horizontal distance is generally worse than the error of a shorter one. An increase in the flying height reduces the effect of the length of the line segment on its standard error.

Standard errors of vertical distances (m)							
σH=0.5 m							
h (m): 3 – 40	σΔH=0.15 m				σΔH=10 m			
	t=15º		t=35º		t=15º		t=35º	
	c=50 mm	c=150 mm	c=50 mm	c=150 mm	c=50 mm	c=150 mm	c=50 mm	c=150 mm
H=200 m	0.47-1.10	0.03-0.12	0.05-0.12	0.01-0.11	0.49-2.28	0.15-2.00	0.16-2.00	0.15-2.00
H=500 m	1.16-1.58	0.08-0.11	0.11-0.13	0.03-0.05	1.16-1.77	0.10-0.81	0.13-0.81	0.07-0.80
H=1000 m	2.31-2.52	0.15-0.17	0.23-0.23	0.06-0.07	2.32-2.55	0.16-0.43	0.23-0.46	0.07-0.41
σH=15 m							
h (m): 3 – 40	σΔH=0.15 m				σΔH=10 m			
	t=15º		t=35º		t=15º		t=35º	
	c=50 mm	c=150 mm	c=50 mm	c=150 mm	c=50 mm	c=150 mm	c=50 mm	c=150 mm
H=200 m	0.52-3.19	0.23-3.00	0.23-3.00	0.23-3.00	0.54-3.77	0.27-3.61	0.27-3.61	0.27-3.61
H=500 m	1.17-1.98	0.12-1.20	0.15-1.21	0.10-1.20	1.17-2.14	0.13-1.45	0.16-1.45	0.11-1.44
H=1000 m	2.32-2.59	0.16-0.62	0.24-0.64	0.08-0.60	2.33-2.62	0.16-0.74	0.24-0.76	0.08-0.72

Table 1. Standard errors of measured vertical distances ranging from 3 m to 40 m

| Standard errors of horizontal distances (m)							
σH=0.5 m							
d (m): 10 – 90	σΔH=0.15 m				σΔH=10 m			
	t=15º		t=35º		t=15º		t=35º	
	c=50 mm	c=150 mm	c=50 mm	c=150 mm	c=50 mm	c=150 mm	c=50 mm	c=150 mm
H=200 m	0.03-0.24	0.03-0.24	0.03-0.24	0.03-0.24	0.50-4.51	0.50-4.51	0.50-4.51	0.50-4.51
H=500 m	0.04-0.13	0.02-0.10	0.04-0.11	0.02-0.10	0.20-1.80	0.20-1.80	0.20-1.80	0.20-1.80
H=1000 m	0.07-0.12	0.03-0.06	0.07-0.10	0.03-0.06	0.12-0.91	0.10-0.90	0.12-0.91	0.11-0.90
σH=15 m							
d (m): 10 – 90	σΔH=0.15 m				σΔH=10 m			
	t=15º		t=35º		t=15º		t=35º	
	c=50 mm	c=150 mm	c=50 mm	c=150 mm	c=50 mm	c=150 mm	c=50 mm	c=150 mm
H=200 m	0.75-6.75	0.75-6.75	0.75-6.75	0.75-6.75	0.90-8.11	0.90-8.11	0.90-8.11	0.90-8.11
H=500 m	0.30-2.70	0.30-2.70	0.30-2.70	0.30-2.70	0.36-3.25	0.36-3.25	0.36-3.25	0.36-3.25
H=1000 m	0.17-1.36	0.15-1.35	0.17-1.35	0.15-1.35	0.19-1.63	0.18-1.62	0.19-1.63	0.18-0.62

Table 2. Standard errors of measured horizontal distances ranging from 10 m to 90 m

4. APPLICATION DEVELOPMENT AND TESTING

The methodology presented for the extraction of vertical and horizontal distances from a single low oblique aerial image was implemented in a Windows console desktop application that was developed in the C++ programming language, using the OpenCV (Open source

Metric Exploitation of a Single Low Oblique Aerial Image (7516)
Styliani Verykokou and Charalabos Ioannidis (Greece)

12/16

FIG Working Week 2015
From the Wisdom of the Ages to the Challenges of the Modern World
Sofia, Bulgaria, 17-21 May 2015

Computer Vision) library and the MPIR (Multiple Precision Integers and Rationals) library. The user of this application is asked to input a single low oblique image, the interior orientation of the camera used for acquiring the image and the flying height. Then, the nadir point is automatically detected and the measuring procedure begins. Specifically, the user is asked to specify the type of the distance that will be measured, that is, a vertical or a horizontal one. The two points that define the distance are approximately measured in the oblique image displayed in a main window and then another window is created, showing a magnified view of the region of interest, so that measurements can be done precisely. After making the photogrammetric measurements in the magnified window, the user is asked to input the elevation difference between the ground nadir point and either the bottom point of the measured vertical distance or one of the endpoints of the measured horizontal line segment. The distance is calculated with the appropriate formula, the result is displayed in the console window and the measuring procedure is continued, until the user terminates the application.

The application was tested using low oblique aerial images taken by a Leica RCD30 Oblique medium format camera system over the city of Zürich from a flying height of about 520 m with a tilt angle of 35°. The images used (9000 x 6732) were free of distortion with a pixel size of 6 μm and correspond to a calibrated focal length of 53 mm. Figures 5 and 6 illustrate some characteristic procedures of the application implemented in the above mentioned oblique data set.
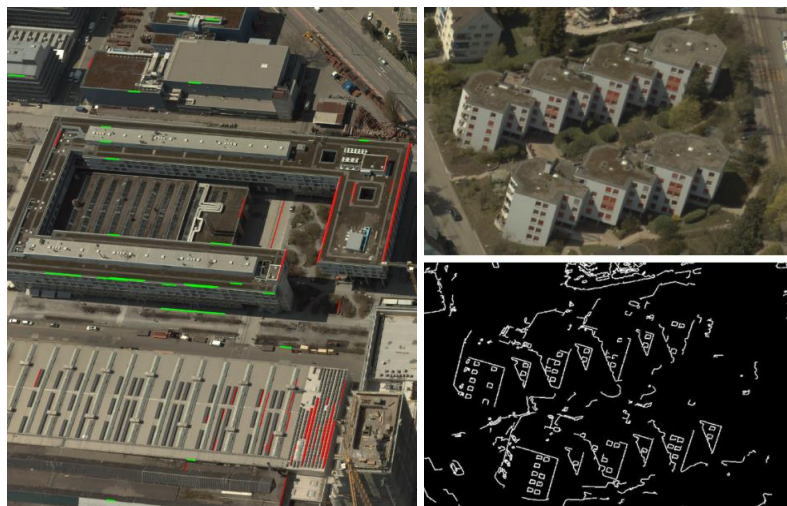

Figure 5. Sets of automatically detected parallel horizontal lines used for the determination of the true horizon line (left) and extraction of Canny edges for the detection of vertical line segments converging to the nadir point (right)

By example it is mentioned that during the process of the true horizon line detection on the image shown in Fig. 6, about 1500 line segments are extracted using the Progressive Probabilistic Hough Transform, out of which about 100 segments are characterized as inliers by RANSAC and are used for the detection of the first horizontal vanishing point via least-squares adjustment and about 40 segments are used for the determination of the second horizontal vanishing point. During the final estimation of the nadir point, about 12000 line segments are extracted using the Progressive Probabilistic Hough Transform, out of which

about 350 line segments converge close to the initial estimation of the nadir point and about 20 of these segments are characterized by RANSAC as inliers and are used for the iterative least-squares estimation of the nadir point. The distance between the initial and the final estimation of the nadir point is about 700 pixels.

15 horizontal line segments ranging from 22 m to 100 m and 10 vertical line segments ranging from 4 m to 20 m were measured using the developed application and the results were compared to stereoscopic measurements using 3 pairs of georeferenced vertical images with a ground sample distance (GSD) of approximately 4 cm, taken with a Z/I DMC II 140 camera. The errors of the measured horizontal distances (d) are almost proportional to the lengths of the measured line segments, ranging from 0.07d to 0.08d, while the errors of the measured vertical distances (h) range from 0.01h to 0.13h. The main parameter that influences the size of the errors is the lack of elevation information for the region vertically under the aerial platform and the region of interest.
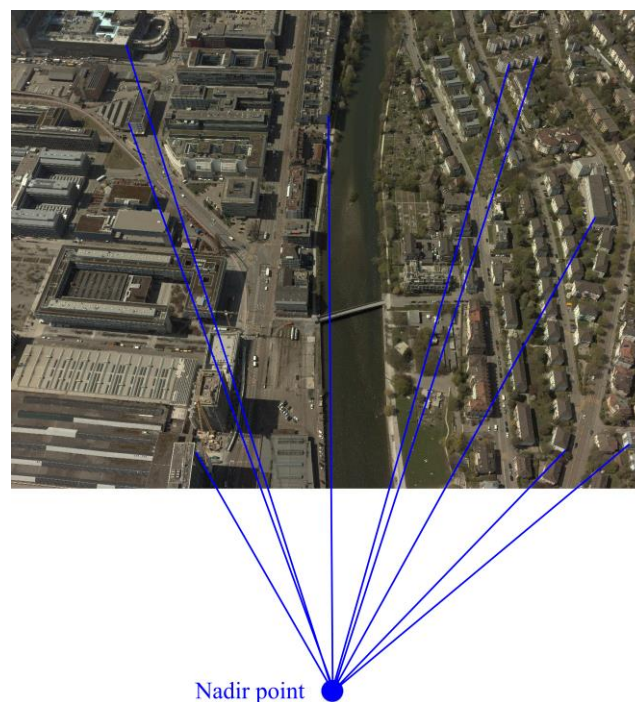
Figure 6. Automatic determination of the nadir point by convergence of vertical lines

5. CONCLUSIONS AND FUTURE WORK

In this paper, a methodology is proposed for the photogrammetric computation of vertical and horizontal distances from single low oblique aerial images. This methodology may be applied in the metric exploitation of a low oblique image taken by a camera of unknown exterior orientation. Furthermore, the effects of different variables, which are involved in the mathematical model used, on the errors of the measured distances are evaluated. The results presented are based on error propagation and were tested in one specific case study. Hence, future work will focus on a more extended analysis of the errors of the measured vertical and horizontal distances by adopting different flight configurations (i.e., different combinations of

the flying height, the camera specifications and the inclination of the camera axis), by considering multiple scenarios as far as the availability of ground elevation data is concerned and by conducting additional field work for the evaluation of the results. Finally, the effects of the earth curvature and the atmospheric refraction on the estimation of distances from oblique images, which are ignored in the present study, will also be evaluated, especially in the case of the metric exploitation of high oblique aerial images, which is another fundamental issue that will be addressed.

ACKNOWLEDGEMENTS

REFERENCES

Baumann, P.R., 2014. *History of Remote Sensing, Aerial Photography*. http://www.oneonta.edu/faculty/baumanpr/geosat2/RS%20History%20I/RS-History-Part-1.htm [Accessed 10 October 2014].

Brown, D.C., 1971. Close-Range Camera Calibration. *Photogrammetric Engineering*, vol. 37, no. 8, pp. 855-866.

Canny, J., 1986. A Computational Approach to Edge Detection. *IEEE Transactions on Pattern Analysis and Machine Intelligence*, vol. PAMI-8, no. 6, pp. 679-698.

Fahsi, A., 1996. *Air Photo Interpretation and Photogrammetry*. http://userpages.umbc.edu/~tbenja1/umbc7/santabar/vol1/lec6/6lecture.html [Accessed 10 October 2014].

Fischler, M., Bolles, R., 1981. Random Sample Consensus: A Paradigm for Model Fitting with Applications to Image Analysis and Automated Cartography. *Communications of the ACM*, vol. 24, no. 6, pp. 381-395.

Gerke, M., 2013. Current Developments in Airborne Oblique Imaging – Systems and Automated Interpretation of Complex Buildings. *Proceedings of 3D-ARCH 2013 – 3D Virtual Reconstruction and Visualization of Complex Architectures*.

Grenzdörffer, G.J., Guretzki, M., Friedlander, I., 2008. Photogrammetric Image Acquisition and Image Analysis of Oblique Imagery – A New Challenge for the DigitalAirborne System PFIFF. *The Photogrammetric Record*, vol. 23, no. 124, pp. 372-386.

Hannavy, J., 2007. *Encyclopedia of Nineteenth-Century Photography*. Routledge, USA.

Matas, J., Galambos, C., Kittler, J., 1998. Progressive Probabilistic Hough Transform. *Proceedings of the British Machine Vision Conference*, pp. 256-265.

Moffitt, F.H., Mikhail, E.M., 1980. *Photogrammetry*. Harper & Row Inc., New York.

Petrie, G., 2008. Systematic Oblique Aerial Photography Using Multiple Digital Cameras. *Proceedings of the VII International Scientific and Technical Conference "From imagery to map: digital photogrammetric technologies"*, pp. 56-57. Moscow, Russia.

Metric Exploitation of a Single Low Oblique Aerial Image (7516)   15/16
Styliani Verykokou and Charalabos Ioannidis (Greece)

FIG Working Week 2015
From the Wisdom of the Ages to the Challenges of the Modern World
Sofia, Bulgaria, 17-21 May 2015

Wolf, P.R., 1983. *Elements of Photogrammetry with Air Photo Interpretation and Remote Sensing*. McGraw-Hill Inc., New York.

BIOGRAPHICAL NOTES

Styliani VERYKOKOU

Surveyor Engineer, PhD candidate at the Lab. of Photogrammetry, School of Rural and Surveying Engineering, National Technical University of Athens, Greece.

She was awarded scholarships and awards by the National Institute of Scholarships of Greece, the Thomaidion Foundation (Greece), the Limmat Foundation (Switzerland), the National Technical University of Athens and the Academy of Athens, as a result of her performance in her studies.

Her research interests lie in the fields of photogrammetry, computer vision, cartography, remote sensing and augmented reality.

Charalabos IOANNIDIS

Professor at the Lab. of Photogrammetry, School of Rural and Surveying Engineering, National Technical University of Athens, Greece, teaching photogrammetry and cadastre. Until 1996 he worked at private sector.

1992-1996: Co-chairman of Commission VI-WG2 'Computer Assisted Teaching' in ISPRS.

1997-2001: Member of the Directing Council of Hellenic Mapping and Cadastral Organization and Deputy Project Manager of the Hellenic Cadastre.

2010-2014: Chair of Working Group 3.2 'Technical Aspects of SIM' of FIG Com 3.

He has authored more than 140 papers in the above fields.

CONTACTS

Styliani Verykokou
School of Rural & Surveying Engineering,
National Technical University of Athens
9 Iroon Polytechniou St.
Athens
GREECE
Email: st.verykokou@gmail.com

Prof. Dr. **Charalabos Ioannidis**
School of Rural & Surveying Engineering,
National Technical University of Athens
Athens
GREECE
Tel. +302107722686
Fax +302107722677
Email: cioannid@survey.ntua.gr
Web site: http://users.ntua.gr/cioannid/

Metric Exploitation of a Single Low Oblique Aerial Image (7516)   16/16
Styliani Verykokou and Charalabos Ioannidis (Greece)

FIG Working Week 2015
From the Wisdom of the Ages to the Challenges of the Modern World
Sofia, Bulgaria, 17-21 May 2015